

# Aspects of nonlocality in atom-photon interactions in a cavity

A. S. Majumdar<sup>\*1</sup> and N. Nayak<sup>†2</sup>

<sup>1</sup>*S. N. Bose National Centre for Basic Sciences, Block JD, Sector III, Salt Lake, Calcutta 700098, India*

<sup>2</sup>*Department of Physics, Texas A&M University, College Station, Texas 77843-4242, USA*

We investigate a Bell-type inequality for probabilities of detected atoms formulated using atom-photon interactions in a cavity. We consider decoherence brought about by both atomic decay, as well as cavity photon loss, and study its quantitative action in diminishing the atom-field and the resultant atom-atom secondary correlations. We show that the effects of decoherence on nonlocality can be observed in a controlled manner in actual experiments involving the micromaser and also the microlaser.

PACS number(s): 03.65.Bz, 42.50.Dv

## I. INTRODUCTION

Nonlocality at the quantum level manifests itself in various kinds of phenomena. The study of this so far, has been predominantly confined to the study of interactions amongst similar kinds of particles, for example, photon-photon interactions or the interaction of subatomic particles among themselves. With the advance of technology over the last several years, it has now become conceivable to investigate a new kind of nonlocality in a controllable fashion, viz., the nonlocality generated through the interaction of distinct entities, like atoms and photons inside a high quality cavity.

The mathematical framework for demonstrating the violation of local realism in quantum mechanics was first provided by Bell [1] through his famous inequalities. This work was subsequently generalized and also extended to consider the interaction of more than two particles [2,3]. A different kind of proof of nonlocality without the use of inequalities, also exists [4]. Furthermore, it has been shown that quantum nonlocality continues to persist even for the case of a large number of particles, or large quantum numbers [5]. This has raised certain questions regarding the issue of the macroscopic or classical limit of quantum mechanics in examples where both the number of particles, and their quantum number is made arbitrarily large [6]. The phenomenon of environment induced decoherence is of direct relevance here. It would be interesting if decoherence could be experimentally controlled and its effect on nonlocality be quantitatively monitored in particular examples of study.

Experimental proposals of demonstrating nonlocality have mostly been concerned with spin-1/2 particles [7], photons [8,9], or mesons [10]. In recent times, several schemes involving two-level Rydberg atoms have been proposed [11,12]. In such schemes two-level rydberg atoms are considered in analogy to the spin system in Bell's original reasoning. The role of the polarization axis of the Stern-Gerlach apparatus used for spin-1/2 systems is played here by the phase of an auxiliary electromagnetic field. The primary advantages of the experiments using atoms, compared to those with photons or spin half particles are two-fold. First, the realization of spacelike separation for Rydberg atoms is easier because of their smaller velocities than photons or electrons. Secondly, the efficiencies of detectors used for the former is much larger in general in comparison with the detectors used for elementary particles. In addition, the interaction of large-sized atoms with the environment can be significant enough to be monitored in certain cases. In fact, in the experimental schemes which involve the interaction of Rydberg atoms with photons in a microwave cavity, dissipation through the loss of cavity photons always occurs. The effect of this is manifested in the form of loss of coherence in the atom-photon interactions. Thus, this is a natural arena to study the effects of decoherence on quantum nonlocality in a quantitative manner.

In this paper we propose a realistic experiment to test Bell's inequality for real micromasers/microlasers by taking experimentally attainable data in the presence of both atomic decay and cavity dissipation under the influence of their respective reservoirs. The approach followed by us enables us to analyze both micromaser as well as microlaser dynamics within the framework of a single formalism in presence of decoherence. Our aim is to study the effects of decoherence on the magnitude of violation of Bell's inequality in an experimentally controllable fashion. As an interesting sidelight, we are also able to demonstrate the effect of decoherence on multiparticle correlations that are

---

<sup>\*</sup>archan@boson.bose.res.in

<sup>†</sup>On leave from S. N. Bose National Centre for Basic Sciences, Calcutta, India.  
nayak@boson.bose.res.in, nayak@atlantic.tamu.edu

a natural outcrop of experimental schemes using microwave cavity that we use for our analysis. In the next section we describe the experimental arrangement and the relevant Bell-type inequality (BI). We wish to emphasize that although the BI used by us is the same as in [12], the cavity dynamics considered by us (the steady-state dynamics is discussed in Section III) differs crucially from the one used in [12]. We are hence able to take into account micromaser dissipation in a more realistic manner, and also analyse the microlaser by incorporating atomic decay. In Section IV we present and discuss our results. Section V is reserved for some concluding remarks.

## II. VIOLATIONS OF BELL'S INEQUALITY IN A MICROCAVITY

We consider the following experimental scenario. A two-level atom initially in its upper excited state  $|e\rangle$  traverses a high-Q single mode cavity. The cavity is in a steady state and tuned to a single mode resonant with the transition  $|e\rangle \rightarrow |g\rangle$ . The emerging single-atom wavefunction is a superposition of the upper  $|e\rangle$  and lower  $|g\rangle$  state, and it leaves an imprint on the photonic wavefunction in the cavity. After leaving the cavity, the atom passes through an electromagnetic field which gives it a  $\pi/2$  pulse the phase of which can be varied for different atoms. The atom then reaches the detector, placed at a sufficient distance, capable of detecting the atom only in the upper or lower state. Thus, the role of the  $\pi/2$  pulse may be considered as a component of the detection mechanism in the experiment [13]. During the whole process, dissipation takes place, and is taken into account. Next, this process is repeated for a similar second atom. The important difference is that the second atom interacts with a photonic wavefunction which has been modified due to the passage of the first atom. There is no direct interaction between the two atoms, although secondary correlations develop between them. In other words, though there is no spatial overlap between the two atoms, the entanglement of their wavefunctions with the cavity photons can be used to formulate local-realist bounds on the detection probabilities for the two atoms [11,12].

The interplay of the atomic statistics with the photonic statistics plays a crucial role in the investigation of non-locality here. The initial state of the cavity is built up by the passage of a large number of atoms, but only one at a time, through it. The pump parameter and the atom-photon interaction time are key inputs for the profile of the resultant photonic wavefunction which in turn governs the nature of entanglement between two successive experimental atoms detected in their upper or lower states by the detector. As stated earlier, dissipation due to the interaction of the pumping atoms with their reservoir, as well as the loss of cavity photons can be controlled, and their effects on the statistics of detected atoms can be studied. The formalism used by us has another generic feature. The effects of decoherence on nonlocality can be studied in context of the micromaser, as well as the microlaser, its optical counterpart.

It is easy to obtain a Bell-type inequality suitable for the scenario considered by us in analogy to Bell's original reasoning. Two level Rydberg atoms are analogous to spin-1/2 systems, and the phase of the electromagnetic field plays the role of the polarization axis of the Stern-Gerlach apparatus used for spin-1/2 systems. In fact, several local realist bounds have earlier been derived to tailor such a situation [11,12]. Let us very briefly describe one such derivation [12] which we shall use in the present analysis. Assigning the value +1 for the atom detected in the upper state  $|e\rangle$ , and -1 for the lower state  $|g\rangle$ , one can in any local realist theory define functions  $f(\phi_1) = \pm 1$ ;  $g(\phi_2) = \pm 1$  describing the outcome of measurement on the atom 1 and 2 when the phase of the electromagnetic field giving  $\pi/2$  pulse to the atoms is set to be  $\phi_1$  and  $\phi_2$  for the respective atoms. The ensemble average for double click events is therefore defined as

$$E^\lambda(\phi_1, \phi_2) = \int d\lambda f(\phi_1)g(\phi_2) \quad (1)$$

where  $\lambda$  is a suitable probability measure on the space of all possible states.

The quantum mechanical expectation value for double click events is calculated from the probabilities of all possible double-click sequences. This is given by

$$\begin{aligned} E(\phi_1, \phi_2) &= P_{ee}(\phi_1, \phi_2) + P_{gg}(\phi_1, \phi_2) \\ &\quad - P_{eg}(\phi_1, \phi_2) - P_{ge}(\phi_1, \phi_2) \end{aligned} \quad (2)$$

where  $P_{eg}(\phi_1, \phi_2)$  stands for the probability that the first atom is found to be in state  $|e\rangle$  after traversing the  $\pi/2$  pulse with phase  $\phi_1$ , and the second atom is found to be in state  $|g\rangle$  with the phase of the  $\pi/2$  pulse being  $\phi_2$  for its case. Defining  $E_0 = E^\lambda(\phi_1 = \phi_2)$  and  $M_0 = P_{ee}(\phi_1 = \phi_2) + P_{gg}(\phi_1 = \phi_2)$ , and assuming perfect detections, it follows that  $E_0 = 2M_0 - 1$ . Further, it is easy to see that  $f(\phi) = +g(\phi)$  with probability  $M_0$ , and  $f(\phi) = -g(\phi)$  with probability  $(1 - M_0)$ . Hence,  $E^\lambda(\phi_1, \phi_2)$  can be written as

$$E^\lambda(\phi_1, \phi_2) = E_0 \int d\lambda f(\phi_1)f(\phi_2) \quad (3)$$

Now, one can define a Bell sum

$$B \equiv |E^\lambda(\phi_1, \phi_2) - E^\lambda(\phi_1, \phi_3)| + \text{sign}(E_0)[E^\lambda(\phi_2, \phi_3) - E_0] \quad (4)$$

It follows immediately from (2-4) that  $B \leq 0$ . In the next section we shall calculate this Bell sum  $B$  and see how it evolves for various values of the cavity parameters. It is convenient to set the values of the phases  $\phi_1 = 0$ ,  $\phi_2 = \pi/3$ , and  $\phi_3 = 2\pi/3$ , as for these values the Bell-type inequality is always violated, i.e.,  $B > 0$  for the case of an idealised micromaser [12].

### III. STEADY-STATE MICROMASER/MICROLASER PHOTON STATISTICS

In realistic situations, one must consider the interacting systems (atoms as well as cavity field) coupled to their respective reservoirs. The couplings are governed by their equations of motion [14],

$$\begin{aligned} \dot{\rho}|_{atom-reservoir} = & -\gamma(1 + \bar{n}_{th})(s^+s^-\rho - 2s^-\rho s^+ + \rho s^+s^-) \\ & - \gamma\bar{n}_{th}(s^-s^+\rho - 2s^+\rho s^- + \rho s^-s^+) \end{aligned} \quad (5)$$

for the atom and

$$\begin{aligned} \dot{\rho}|_{field-reservoir} = & -\kappa(1 + \bar{n}_{th})(a^\dagger a \rho - 2a \rho a^\dagger + \rho a^\dagger a) \\ & - \kappa\bar{n}_{th}(a a^\dagger \rho - 2a^\dagger \rho a + \rho a a^\dagger) \end{aligned} \quad (6)$$

for the field.  $\rho$  is the reduced density operator obtained after tracing over the reservoir.  $\gamma$  and  $\kappa$  are the decay constants for the atom and the field respectively.  $\bar{n}_{th}$  is the average photon number representing the reservoir.  $s^+$  and  $s^-$  are the usual Pauli operators for the pseudo-spin representation of the two-level model of the atom.  $a(a^\dagger)$  is the photon annihilation (creation) operator.

The dynamics we are interested in, involves two-level atoms steamed into a single mode cavity in such a way that there is at most one atom in the cavity at any time. Thus we have sequences of events (atom-field interactions) taking place randomly, but with each event of a fixed duration  $\tau$ . This interaction is governed by

$$\dot{\rho}|_{atom-field} = -i[H, \rho] \quad (7)$$

where  $H = g(s^+a + s^-a^\dagger)$  is the well known Jaynes-Cummings [15] Hamiltonian with  $g$  being the coupling constant.

Thus, we have to solve the equation of motion

$$\dot{\rho} = \dot{\rho}|_{atom-reservoir} + \dot{\rho}|_{field-reservoir} + \dot{\rho}|_{atom-field} \quad (8)$$

where the terms on the r.h.s. are the r.h.s' of (5), (6) and (7) respectively. For the duration between two events, we have to solve the equation of motion (6) only.

The steady-state photon statistics of the cavity field undergoing such dynamics has been derived in [16]. In the cavity photon number representation, the probabilities  $P_n = \langle n | \rho_f^{(ss)} | n \rangle$  are given by

$$P_n = P_0 \prod_{m=1}^n v_m \quad (9)$$

$P_0$  is obtained from the normalisation  $\sum_{n=0}^{\infty} P_n = 1$ . The  $v_n$  are given by the continued fractions

$$v_n = f_3^{(n)} / (f_2^{(n)} + f_1^{(n)} v_{n+1}) \quad (10)$$

with  $f_1^{(n)} = (Z_n + C_n)/\kappa$ ,  $f_2^{(n)} = -2N + (Y_n + B_n)/\kappa$  and  $f_3^{(n)} = -(X_n + A_n)/\kappa$ .  $\kappa$  is the cavity bandwidth and  $N = R/2\kappa$  is the number of atoms passing through the cavity in a photon lifetime.  $A_n = 2n\kappa\bar{n}_{th}$ ,  $B_n = -2\kappa(n + \bar{n}_{th} + 2n\bar{n}_{th})$  and  $C_n = 2(n + 1)(\bar{n}_{th} + 1)\kappa$ .  $X_n$ ,  $Y_n$  and  $Z_n$  are given by

$$X_n = R \sin^2(g\sqrt{n}\tau) \exp\{-[\gamma + (2n - 1)\kappa]\tau\} \quad (11)$$

$$\begin{aligned}
Y_n = & \frac{1}{2}R \left( \{2\cos^2[g\sqrt{n+1}\tau] - \frac{1}{2}(\gamma/\kappa + 2n + 1) \right. \\
& + F_1(n-1)\} \exp\{-[\gamma + (2n+1)\kappa]\tau\} + [\frac{1}{2}(\gamma/\kappa + 2n + 1) \right. \\
& \left. \left. - F_2(n-1)\} \exp\{-[\gamma + (2n-1)\kappa]\tau\} \right),
\end{aligned}$$

and

$$\begin{aligned}
Z_n = & \frac{1}{2}R \left( [\frac{1}{2}(\gamma/\kappa + 2n + 3) + F_2(n)] \exp\{-[\gamma + (2n+1)\kappa]\tau\} \right. \\
& \left. - [\frac{1}{2}(\gamma/\kappa + 2n + 3) + F_1(n)] \exp\{-[\gamma + (2n+3)\kappa]\tau\} \right)
\end{aligned}$$

$\gamma$  represents reservoir induced spontaneous emission from the upper to the lower masing level. The functions  $F_i$  are

$$\begin{aligned}
F_i(n) = & \frac{\kappa/4g}{(\sqrt{n+2} - \sqrt{n+1})^2} \\
& \left[ \frac{\gamma}{\kappa}(\sqrt{n+2} - \sqrt{n+1}) \sin(2g\sqrt{m}\tau) - \frac{\gamma}{g} \cos(2g\sqrt{m}\tau) \right. \\
& \left. - [2n+3 + 2\sqrt{(n+1)(n+2)}](\sqrt{n+2} - \sqrt{n+1}) \sin(2g\sqrt{m}\tau) \right] \\
& + \frac{\kappa/4g}{(\sqrt{n+2} + \sqrt{n+1})^2} \\
& \left[ \pm \frac{\gamma}{\kappa}(\sqrt{n+2} + \sqrt{n+1}) \sin(2g\sqrt{m}\tau) - \frac{\gamma}{g} \cos(2g\sqrt{m}\tau) \right. \\
& \left. \mp [2n+3 - 2\sqrt{(n+1)(n+2)}](\sqrt{n+2} + \sqrt{n+1}) \sin(2g\sqrt{m}\tau) \right] \tag{12}
\end{aligned}$$

where  $m = n+2$  and  $n+1$  for  $i = 1$  and  $2$ , respectively, with the upper sign for  $i = 1$ .

The experimental atoms on which we plan to test the Bell's inequality (BI), encounter this steady state radiation field  $\rho_f^{(ss)}$ . The atom-field interaction is, as mentioned earlier governed by the Jaynes-Cummings Hamiltonian  $H$ . After interaction with the cavity, the first experimental atom emerges in a superposition of the upper ( $|e\rangle$ ) and the lower ( $|g\rangle$ ) states and experiences a  $\pi/2$  pulse with phase  $\phi_1$ . The probability of detection of the atom in the upper state  $|e\rangle$  and the lower state  $|g\rangle$  can be written respectively as

$$\begin{aligned}
P_e &= \text{Tr}_{\text{f}} \mathcal{P}_e \\
P_g &= \text{Tr}_{\text{f}} \mathcal{P}_g \tag{13}
\end{aligned}$$

with

$$\begin{aligned}
\mathcal{P}_e &= \frac{1}{2}[\mathcal{A}\rho_f^{(ss)}\mathcal{A}^\dagger + \mathcal{D}\rho_f^{(ss)}\mathcal{D}^\dagger - \{e^{-i\phi_1}\mathcal{A}\rho_f^{(ss)}\mathcal{D}^\dagger + e^{i\phi_1}\mathcal{D}\rho_f^{(ss)}\mathcal{A}^\dagger\}] \\
\mathcal{P}_g &= \frac{1}{2}[\mathcal{A}\rho_f^{(ss)}\mathcal{A}^\dagger + \mathcal{D}\rho_f^{(ss)}\mathcal{D}^\dagger + \{e^{-i\phi_1}\mathcal{A}\rho_f^{(ss)}\mathcal{D}^\dagger + e^{i\phi_1}\mathcal{D}\rho_f^{(ss)}\mathcal{A}^\dagger\}] \tag{14}
\end{aligned}$$

where trace is taken over the cavity field and the operators  $\mathcal{A}$  and  $\mathcal{D}$  are given by

$$\begin{aligned}
\mathcal{A} &= \cos(gt\sqrt{a^\dagger a + 1}) \\
\mathcal{D} &= -ia^\dagger \frac{\sin(gt\sqrt{a^\dagger a + 1})}{\sqrt{a^\dagger a + 1}} \tag{15}
\end{aligned}$$

After the passage of the first atom through the cavity and its detection in, for example, the state  $|e\rangle$ , the second atom encounters the cavity field with density operator  $\rho_f^{(2)}$  given by

$$\rho_f^{(2)} = [\mathcal{A}\rho_f^{(ss)}\mathcal{A}^\dagger + \mathcal{D}\rho_f^{(ss)}\mathcal{D}^\dagger - \{e^{-i\phi_1}\mathcal{A}\rho_f^{(ss)}\mathcal{D}^\dagger + e^{i\phi_1}\mathcal{D}\rho_f^{(ss)}\mathcal{A}^\dagger\}] \tag{16}$$

(since  $\text{Tr}_{\text{f}}\mathcal{P}_e = 1/2$ ). The phase of the  $\pi/2$  pulse is set to  $\phi_2$  for the second atom.  $\mathcal{P}_e$  for the second atom is given by

$$\mathcal{P}_e^{(2)} = \frac{1}{2}[\mathcal{A}\rho_f^{(2)}\mathcal{A}^\dagger + \mathcal{D}\rho_f^{(2)}\mathcal{D}^\dagger - \{e^{-i\phi_1}\mathcal{A}\rho_f^{(2)}\mathcal{D}^\dagger + e^{i\phi_1}\mathcal{D}\rho_f^{(2)}\mathcal{A}^\dagger\}] \quad (17)$$

The conditional probability  $P_{ee}(\phi_1, \phi_2)$  is thus given by

$$P_{ee}(\phi_1, \phi_2) = \text{Tr}_{\text{f}}\mathcal{P}_e^{(2)} \quad (18)$$

$P_{gg}$  is obtained similarly, and using the relations  $E(\phi_1, \phi_2) = 2P(\phi_1, \phi_2) - 1$  and  $P(\phi_1, \phi_2) = P_{ee}(\phi_1, \phi_2) + P_{gg}(\phi_1, \phi_2)$  one obtains the values of  $E$  in the Bell sum (4). We perform this exercise numerically with the values of the phases in the Bell sum (4) set to  $\phi_1 = 0$ ,  $\phi_2 = \pi/3$ , and  $\phi_3 = 2\pi/3$ .

It will be appropriate to mention here that although decoherence effects are inherent in the build up of the cavity field to its steady state since it encounters a large number of atoms over the time required for the steady state to be reached, the dynamics of a single experimental atom interacting with this field for a short duration will be unaffected by the decoherence effects, as has been observed in the cavity-QED of Jaynes-Cummings interaction [17]. It was shown there that typical durations of atom-field interactions in realistic environments can be as large as  $t \sim 10/g$  up to which decoherence effects are insignificant. We again stress here that even though the individual atom-field interaction time in the dynamics of the cavity field, pumped repeatedly with atoms, is uniformly of this order, the dissipative forces there play a crucial role due to the number of atoms ( $\gg 1$ ) and the time ( $\gg 10/g$ ) involved in reaching the steady state. The same argument applies to the case of atomic damping, as well. Indeed, we keep the above argument in mind in our choice of parameters while calculating the probabilities in the Bell sum (4).

The micromaser model considered by us differs crucially from that in [12] because in the latter model cavity dissipation is neglected whenever an atom is present in the cavity. Our model takes into account dissipation even during the short atom-field interaction times. This *a priori* small effect on cavity photon statistics gets magnified due to the requirement of passage of a large number of atoms through the cavity for it to reach its steady state. Thus, as expected, the resultant steady-state photon statistics in our model is clearly different from the one used in [12]. Let us again emphasize, that although the Bell's inequality (BI) we propose to test is the same as in [12], our cavity dynamics are fundamentally different: (a) our micromaser model (discussed in detail in [16]) is more realistic, and (b) we are also able to analyse the microlaser by incorporating atomic decay.

#### IV. EFFECTS OF CAVITY DISSIPATION AND ATOMIC DECAY ON THE BELL SUM

In the previous section we have presented steady-state cavity dynamics describing both the micromaser as well as the microlaser within a unified framework. However, their distinctive features are manifested in the choice of parameters which we use below to study the violation of BI in both separately. Our choice of different sets of experimentally attainable parameters for both the micromaser and the microlaser is motivated by the following considerations. Recall that the experimental atoms are pumped into the cavity with steady-state photon statistics at such a rate that at most one atom is present in the cavity at any time. So, there are two situations: (a) atom present in the cavity, and (b) cavity empty of atom. Whatever be the situation, cavity dissipation, i.e., the interaction of the cavity mode with its reservoir continues uninterrupted. This process is of crucial importance in micromaser dynamics, and has been discussed in detail in [16]. However, while considering micromaser dynamics, one can safely set atomic decay to zero. This is because the Rydberg levels involved in the micromaser have a lifetime of about  $0.2s$ , whereas the atomic flight time through the cavity (atom-field interaction time) is typically  $35\mu s$ . We present the variation of the Bell sum  $B$  with respect to the parameter  $D$  (which is nothing but the Rabi angle  $\phi$  scaled by the pump rate  $N$ , i.e.,  $D = \phi\sqrt{N}$ ) for the case of the micromaser in Figure 1.

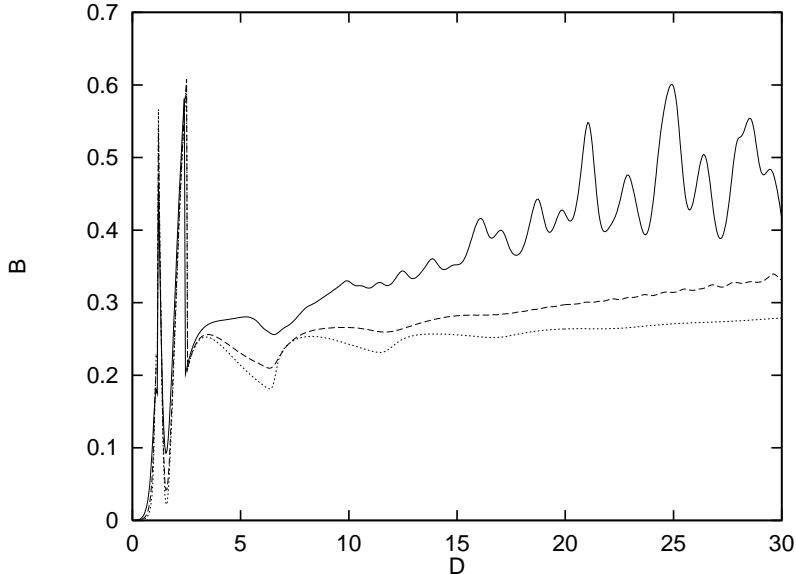


FIG. 1.

Violation of Bell's inequality in a micromaser [20]. Atoms in the upper of the two Rydberg levels are streamed into a cavity, one at a time, in such a way that the flight time of an atom  $\tau$  is much shorter than the lifetime of the long-lived Rydberg levels. Hence, we set the atomic decay constant  $\gamma = 0$ . The average thermal photons  $\bar{n}_{th} = 0.15$  in the cavity represent its temperature at  $0.5K$ . The leakage of the cavity photons is represented by  $\kappa/g = 0.1 \times 10^{-6}$ . The pump rate  $N$ , the number of individual atoms that pass through the cavity in a photon lifetime, = 20 (full), 50 (broken), and 100 (dotted).  $D = \phi\sqrt{N}$  where the Rabi angle  $\phi = g\tau$ . The parameters are very close to the experimental data in [20].

Our results show clearly that the Bell sum reflecting the degree of nonlocality exhibited in the atom-atom secondary correlations depends heavily on cavity dissipation. In particular, it is seen that the value of Bell sum  $B$  decreases with the increase of pump rate  $N$  for a large range of interaction times  $\tau$ . This can be understood from the way dissipative effects creep into the dynamics through two parameters  $N$  and  $\tau$  [16]. The genesis of atom-photon and the resultant atom-atom entanglement competes with decoherence in an interesting fashion over time. For shorter values of single atom interaction times we find that the correlations build up sharply with  $\tau$ , and the peak value of  $B$  signifying maximum violation of BI is larger for higher values of  $N$ , (as a magnification of Figure 1 reveals). The maximum violation (the value of  $B$  at its second peak) is 0.5812 for  $N = 20$  (full line), 0.6079 for  $N = 50$  (broken) and 0.6241 for  $N = 100$  (dotted) (See Figure 2 where we magnify the curves in the region  $D \leq 5$  of Figure 1 for a clear display of these peaks). This feature is a curious example of multiparticle induced nonlocality. It is analogous to the enhancement of nonlocality for multiparticle systems, and is in conformity with the mathematical demonstration of larger violation of BI with increase in the number of particles involved [5,6]. For short interaction times, naturally the effects of decoherence are too small to affect the correlations. One noticeable feature in Figure 1 is the structures for low values of  $N$  (full line). This originates from “trapped state” dynamics of photonic statistics [16,18] where it has been shown that dissipative effects gradually wash out such states, as can be seen from the broken and dotted lines.

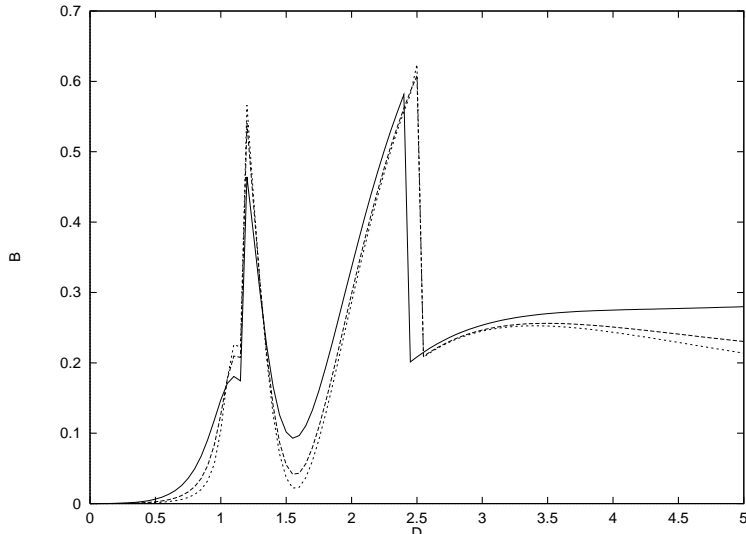


FIG. 2. Enhancement of nonlocality for increased  $N$  in the micromaser. The maximum value of  $B$  is 0.5812 for  $N = 20$  (full line), 0.6079 for  $N = 50$  (broken), and 0.6241 for  $N = 100$  (dotted).

Let us now consider the violation of BI in the microlaser. It is well known that atomic decay is an important factor in the microlaser where atomic levels at optical frequencies are involved. Although decay is unimportant for the dynamics of a single atom interacting with the field up to a certain interaction time, its accumulated effect for a large number of atoms is crucial for the evolution of the microlaser field to a steady state. Furthermore, the interaction time of the atom with the  $\pi/2$  pulse (in this case it is  $gt = \pi/2$ ) is far less compared to even individual atom-field interaction times of interest in microlaser dynamics. For this reason the effect of atomic decay can be neglected during interaction of the atom with the  $\pi/2$  pulse. Our results for the microlaser are shown in Figure 3.

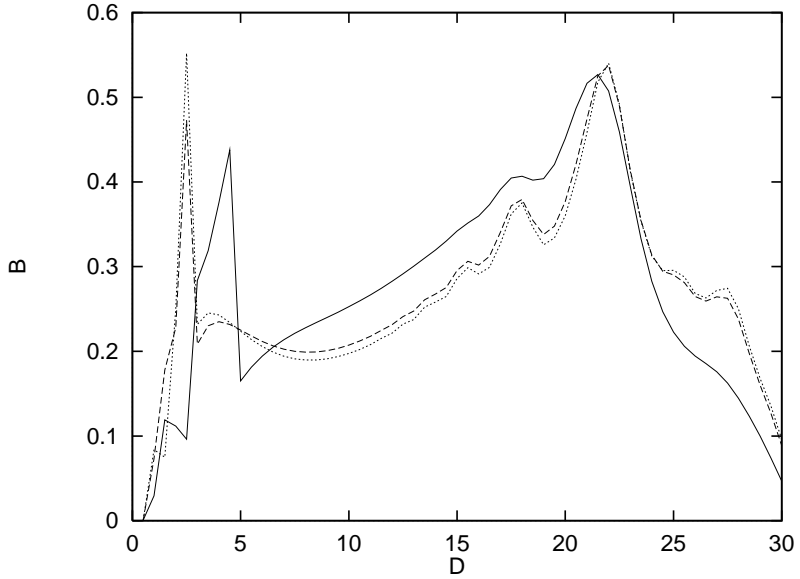


FIG. 3.

Demonstration of nonlocality in a microlaser, the optical counterpart of the micromaser. The results of our numerical simulations can be tested in a microlaser of the type in [21]. Atomic levels having transition frequency in the optical regime have shorter lifetimes compared to Rydberg levels, and hence, we set  $\gamma/g = 0.1$ . At optical frequencies, thermal photons are very close to zero, and thus we take  $\bar{n}_{th} = 0$ .  $N = 100$ . The cavity leakage rate is  $\kappa/g = 0.01$  (full), 0.001 (broken) and 0.0001 (dotted).

The effect of decoherence (cavity leakage rate  $\kappa/g$ ) on the violation of BI is clearly seen in the microlaser. One can

check, similar to the case of the micromaser that the value of Bell sum  $B$  decreases with the increase of pump rate  $N$  for a large range of interaction times  $\tau$ . But in case of the microlaser, atomic damping  $\gamma$  is a dominating factor, in contrast to the cavity photon loss in the micromaser. This makes the Bell sum fall off rapidly for large values of  $\tau$ . The second peak in  $B$  however, is a consequence of the Jaynes-Cummings dynamics and survives such dissipation [19].

## V. CONCLUSIONS

To summarize, we have shown that a demonstration of nonlocality, encompassing several of its varied aspects in atom-photon interactions in cavities and the effects of decoherence on it, can be possible in experimental set-ups already in operating conditions for the micromaser [20], as well as for the microlaser [21]. The formalism chosen enables us to consider the steady-state dynamics of both the micromaser as well as the microlaser in the presence of atomic decay and cavity dissipation within a unified framework. Their distinguishing features are brought about by the different values of the parameters chosen to analyze the violation of BI in them separately. Certain notable features, such as enhancement of nonlocality for increased number of atoms, when decoherence effects are small, can be observed. We have seen how such features can be quantitatively monitored by control of decoherence. In an actual experiment, certain points have to be borne in mind. A few atoms may go undetected between two detector clicks. However, the steady state nature of the cavity field contributes to making the effect of this on the Bell sum insignificant compared to the effect of decoherence which we have probed in detail. Finally, the observed magnitude of violation of BI would be brought down by finite detector efficiency. Nevertheless, our selection of the particular type of BI [12], and the phases of  $\phi$ , ensure that this BI is always violated for the range of parameters chosen irrespective of the efficiency factor of the detector, which can in any case be accounted for easily by the introduction of appropriate scaling factors in the expressions of the various probabilities appearing in the Bell sum.

- [1] J. S. Bell, *Physics* **1**, 195 (1964).
- [2] See, for example, “Quantum mechanics versus local realism”, ed. F. Selleri (Plenum, New York, 1988).
- [3] J. F. Clauser, M. A. Horne, A. Shimony, and R. A. Holt, *Phys. Rev. Lett.* **23**, 880 (1969); D. M. Greenberger, M. A. Horne, A. Shimony and A. Zeilinger, *Am. J. Phys.* **58**, 1131 (1990).
- [4] L. Hardy, *Phys. Rev. Lett.* **71**, 1665 (1993); S. Goldstein, *Phys. Rev. Lett.* **72**, 1951 (1994).
- [5] A. Garg and N. D. Mermin, *Phys. Rev. Lett.* **49**, 901 (1982); N. D. Mermin, *Phys. Rev. Lett.* **65**, 1838 (1990); S. M. Roy and V. Singh, *Phys. Rev. Lett.* **67**, 2761 (1991); M. D. Reid and W. J. Munro, *Phys. Rev. Lett.* **69**, 997 (1992); A. Peres, *Phys. Rev. A* **46**, 4413 (1992); G. S. Agarwal, *Phys. Rev. A* **47**, 4608 (1993).
- [6] D. Home and A. S. Majumdar, *Phys. Rev. A* **52**, 4959 (1995).
- [7] M. Lamehi-Rachti and W. Mittig, *Phys. Rev. D* **14**, 2543 (1976); J. F. Clauser and A. Shimony, *Rep. Prog. Phys.* **41**, 1881 (1978); Z. Y. Ou and L. Mandel, *Phys. Rev. Lett.* **61**, 50 (1988); T. E. Kiess, Y. H. Shih, A. V. Sergienko and C. O. Alley, *Phys. Rev. Lett.* **71**, 3893 (1993).
- [8] A. Aspect, P. Grangier and G. Roger, *Phys. Rev. Lett.* **49**, 91 (1982); A. Aspect, J. Dalibard and G. Roger, *Phys. Rev. Lett.* **49**, 1804 (1982).
- [9] P. D. Drummond, *Phys. Rev. Lett.* **50**, 1407 (1983); P.G. Kwiat et al., *Phys. Rev. Lett.* **75**, 4337 (1995).
- [10] A. Datta and D. Home, *Found. Phys. Lett.* **4**, 165 (1991); R. A. Bartlmann and W. Grimus, *Phys. Lett. B* **392**, 426 (1997).
- [11] S. J. D. Phoenix and S. M. Barnett, *J. Mod. Opt.* **40**, 979 (1993); M. Freyberger et al., *Phys. Rev. A* **53**, 1232 (1996); E. Hagley et al., *Phys. Rev. Lett.* **79**, 1 (1997); A. Jabs, quant-ph/9811042.
- [12] M. Löffler, B.-G. Englert and H. Walther, *Appl. Phys. B* **63**, 511 (1996).
- [13] B. -G. Englert, T. Gantsog, A. Schenzle, C. Wagner, and H. Walther, *Phys. Rev. A* **53**, 4386 (1996).
- [14] See, for example, W. H. Louisell, “Quantum statistical properties of radiation” (Wiley, New York, 1973).
- [15] E.T.Jaynes and F.W.Cummings, *Proc. IEEE* **51**, 89 (1963).
- [16] N. Nayak, *Opt. Commun.* **118**, 114 (1995).
- [17] N. Nayak, R. K. Bullough, B. V. Thompson and G. S. Agarwal, *IEEE J. Quant. Electron.* **QE-24**, 1331 (1988).
- [18] P. Filipowicz, J. Javanainen and P. Meystre, *Phys. Rev. A* **34**, 3077 (1986); L. A. Lugiato, M. O. Scully and H. Walther, *Phys. Rev. A* **36**, 740 (1987).
- [19] N. Nayak, *Opt. Lett.* **24**, 13 (1999).
- [20] One-atom maser (micromaser) action has been observed in, G. Rampe, F. Schmidt-Kaler and H. Walther, *Phys. Rev. Lett.* **64**, 2783 (1990).

[21] K. An, J. J. Childs, R. R. Dasari, and M. S. Feld, Phys. Rev. Lett. **73**, 3375 (1994). Uniform atom-field coupling constant in the cavity, an essential feature of the dynamics [19] considered here, has been obtained by them in, K. An, R. R. Dasari and M. S. Feld, Opt. Lett. **22**, 1500 (1997). Our present investigation shows that nonlocality can be demonstrated in such a device with strictly single-atom events. The MIT group is near attaining such events, R. R. Dasari (Private communication).